Article:
Tozer, G.M., Prise, V.E. and Cunningham, V.J. (2016) Quantitative estimation of tissue blood flow rate. Methods in Molecular Biology, 1430. pp. 265-281. ISSN: 1064-3745

https://doi.org/10.1007/978-1-4939-3628-1_18

The final publication is available at Springer via http://dx.doi.org/10.1007/978-1-4939-3628-1_18.

Quantitative Estimation of Tissue Blood Flow Rate

Gillian M Tozer, Vivien E Prise and Vincent J Cunningham

Abstract

The rate of blood flow through a tissue (*F*) is a critical parameter for assessing the functional efficiency of a blood vessel network following angiogenesis. This chapter aims to provide the principles behind the estimation of *F*, how *F* relates to other commonly used measures of tissue perfusion and a practical approach for estimating *F* in laboratory animals, using small readily diffusible and metabolically inert radio-tracers. The methods described require relatively non-specialized equipment. However, the analytical descriptions apply equally to complementary techniques involving more sophisticated non-invasive imaging. Two techniques are described for the quantitative estimation of *F* based on measuring the rate of tissue uptake following intravenous administration of radioactive iodo-antipyrine (or other suitable tracer). The Tissue Equilibration Technique is the classical approach and the Indicator Fractionation Technique, which is simpler to perform, is a practical alternative in many cases. The experimental procedures and analytical methods for both techniques are given, as well as guidelines for choosing the most appropriate method.

Key Words: backflux, blood flow rate, cannulation, distribution volume, indicator fractionation, iodo-antipyrine, partition coefficient, radiotracer, tissue equilibration

1. Introduction

The maturation phase of angiogenesis results in a functional blood vessel network. In established tumours, this network is abnormal but nevertheless sufficient to support tumour growth and metastasis. Blood flow rate through the vascular network is a measure of its functional efficiency, knowledge of which is central to understanding the angiogenic process. Its quantitative estimation provides the basis for determining oxygen, nutrient and drug delivery to tissue (see **Note 1**). In pathological angiogenesis, such as in tumours, blood flow rate is the most sensitive and relevant pharmacodynamic end-point for determining the efficacy of drugs designed to disrupt blood vessel function. Therefore, estimation of blood flow rate is essential for both basic studies of the angiogenic process and applied studies of the effects of therapy. This chapter aims to provide the principles behind, and a practical approach to, the quantitative estimation of blood flow rate in experimental mice and rats .

Blood flow rate is the rate of delivery of arterial blood to the capillary beds within a particular mass of tissue. It is typically measured in units of mls of blood per g of tissue per minute ((ml blood)•(g tissue)-^{1}•min^{-1}), or, alternatively, per unit volume of tissue ((ml blood)•(ml tissue)$^{-1}$•min^{-1}).

The average time taken for blood to pass through a particular capillary bed (capillary mean transit time (τ) is the parameter that relates tissue blood flow rate

(*F in ml•g^{-1}•min^{-1}*) to fractional blood volume of the tissue (*V in ml•g^{-1}*). This classical relationship is known as the *central volume principle* (1):

$\tau = V/F$ ……*Equation 1*

For different tissues, *F* can vary widely, for example it is approximately 0.1 ml•g^{-1}•min^{-1} in rat skin and 4.0 ml•g^{-1}•min^{-1} in rat kidney. From Equation 1 and using a value for *V* of 0.03 ml•g^{-1} for skin and 0.06 ml•g^{-1} for kidney, τ is approximately 18 s and 0.9 s respectively for these tissues. From *Equation 1*, τ is only indirectly proportional to *F*, if *V* is constant, and so neither τ nor *V* can be used to estimate *F* unless they are both measured simultaneously. The same considerations apply to parameters related to τ, such as *red blood cell velocity* (RBC velocity) and the *blood supply time* (*BST*); see below.

In order to estimate *F*, the most accurate approach is to measure the rate of delivery of an agent carried to the tissue by the blood. A contrast agent is injected into the blood-stream, its concentration time-course in arterial blood (input function) together with the kinetics of its uptake into tissue (tissue response function) are measured. *F* is then estimated from a mathematical model relating the tissue response function to the input function (see below). The contrast agent can be radio-active, whereby tissue concentrations can be measured by gamma or scintillation counting or by an external imaging system (e.g. a positron emitter for positron emission tomography). Alternatively, a contrast agent that is suitable for external magnetic resonance imaging, computed tomography or ultrasound imaging can be used. Radio-active agents have the advantage that they can be

administered at true tracer concentrations, therefore not interfering with physiological processes, and they do not necessarily need sophisticated imaging technology.

Some common methods for determining blood perfusion parameters are given below, most of which do not provide fully quantitative estimates of the blood flow rate, *F*:

1. Intravital microscopy (see Chapters X and X) is a specialised technique that enables direct visualisation of tissue microcirculation, usually via surgically implanted transparent chambers or single-sided windows. This enables measurement of RBC velocity ($\mu m \bullet s^{-1}$) in individual capillaries, as well as the blood supply time (BST, defined below). RBC velocity is measured either by directly tracking individual fluorescently labelled red blood cells through vessel segments (2) or matching the interference patterns of light reaching a camera through a slit system (3). Modern computing techniques now enable comparison of optical signals at individual spatial locations with those in neighbouring locations over time, so that 2-dimensional maps of both speed and direction of blood flow can be constructed, based on similar principles to the classical slit system approach (4). Measurements can be combined with measurements of red cell flux (number of red blood cells traversing a vessel segment per unit time) to calculate microvascular haematocrit (5) or with morphological measurements of individual blood vessel segments to obtain each segment's *volume flow rate (F_{seg}),* which assumes that RBCs are

traveling with the bulk plasma flow (6). Measurement of BST has been carried out in intravital studies of tumours, from images of the tumour vascular network over time, following the intravenous injection of a fluoresecent marker such as TRITC-dextran (7). For each pixel of the vascular image, BST is defined as the time difference between the frame showing maximum fluorescence intensity and the frame showing maximum fluorescence intensity in a tumour-supplying artery, during a short timescale following intravenous injection. Both RBC and BST provide functional information on tumour perfusion but are not directly related to *F,* as discussed above.

2. Laser Doppler flowmetry (LDF) provides a means of estimating *relative changes* in red cell velocity e.g. following treatment, via surface or tissue-inserted probes. This measures a frequency shift in light reflected from moving red cells, which is a measure of average red cell velocity (8). Again, it should be noted that changes in red cell velocity may not accurately reflect changes in *F.*
3. The fluorescent DNA-binding dye, Hoechst 33342, and certain carbo-cyanine dyes are examples of rapidly binding agents that have been used to determine a ‘perfused vascular volume’ (as a fraction of the total tissue volume) rather than blood flow rate *per se*. This method has been used especially in tumour studies (9, 10)}. In this case, tissues are excised after several circulation times, following intra-venous injection of the dye, and functional vessels appear in tissue sections as fluorescent halos. Alternatively, a fluorescently tagged lectin that rapidly binds to endothelial cells *in vivo* can be used (11).

Conventional Chalkley point counting (12, 13) or image analysis provides the fractional tissue volume occupied by fluorescence. This is a useful measure of vascular function in many circumstances but is insensitive because it cannot discriminate between perfused vessels with different flow rates.

4. For contrast agents that are confined to the blood-stream, methods based on Equation 1 can be used to calculate F (14). However, this is difficult in practice because τ is only a few seconds, requiring highly sensitive techniques for its measurement. Radioactive or coloured 'microspheres' of diameters around 15 - 25 μm are a special class of contrast agents that are confined to the blood-stream because they should be trapped on first-pass through tissue. Therefore, following injection directly into a major artery, they distribute to tissues in direct proportion to the fraction of the cardiac output received by the tissues, enabling calculation of blood flow rate (15). With this technique, care needs to be taken to ensure adequate mixing of the microspheres in the arterial blood (which is challenging in mice, for instance) and enough microspheres are lodged in the tissue regions of interest to obtain statistical validity. In the case of tumours, care needs to be taken to determine and correct for microspheres that are re-circulated due to lack of trapping in large diameter vessels (16, 17).

5. The principles used to calculate blood flow rate using microspheres can sometimes be used even when the indicator crosses the vascular wall into the tissue and re-circulates after the first pass through the tissue. If the tissue concentration of the indicator reaches a constant level that is maintained for

the first minute or so after injection, this indicates that the extraction fraction by the tissue is equal to that of the whole body (18). The fractional uptake of the indicator into the tissue must therefore equate to the blood flow fraction of the cardiac output received. In the original description of the technique, potassium and rubidium chloride behaved as 'pseudo-microspheres' in most normal tissues, with the notable exception of brain (18).

6. Small, lipid-soluble, metabolically inert molecules, which rapidly cross the vascular wall and diffuse through the extra-vascular space, are also useful as blood flow markers. In this case, the fraction of marker crossing the capillary vascular wall from the blood in a single pass through the tissue (extraction fraction, *E*) is close to 1.0 and for fully perfused tissue the accessible volume fraction (α) of the tissue is also close to 1.0. The inert radioactive gas, ^{133}Xenon, or hydrogen can be administered by inhalation (19, 20). However, safety issues with ^{133}Xenon and the necessity for tissue insertion of polarographic electrodes for hydrogen have limited their use. A practical approach, which has utility for accessing the spatial heterogeneity of tissue blood flow rate, is the intravenous administration of a small, lipid soluble, inert molecule dissolved in saline. In this case, net uptake rate into tissue over a short time (seconds) after intra-venous injection is determined primarily by blood flow rate. Methods for quantitative estimation of tissue blood flow rate and related parameters using these agents are described below (see **Note 2**).

2. Materials

2.1 Radioactive tracer preparation

1. Any small, lipid soluble molecule that can be suitably labelled and is not metabolized in tissue over the short time of the experiment can be used. Suitable radio-isotopes include ^{125}I and ^{14}C, where tissue and blood counts can be obtained using standard techniques and autoradiography /phosphor imaging can be applied if spatial variation in blood flow rate across a tissue of interest is required (see **Note 3**).
2. One that has been used commonly for both normal tissue studies (primarily brain (21)) and tumour studies (22) is iodo-antipyrine (IAP) (Figure 1). ^{125}I-IAP is commercially available, for example from MP Biomedicals and ^{14}C-IAP (4-Iodo[*N-methyl* -14 C]antipyrine) from PerkinElmer. Alternatively, a technique for labelling IAP with ^{125}I is described by Trivedi (23) (see **Note 4**).

2.2 Animal preparation

Large vessel cannulation is required for intravenous administration and arterial blood sampling. Materials required:

1. general anaesthetic
2. heparinised saline for cannulae (add 0.3ml of 1000U/ml heparin to 10ml saline)
3. general surgical equipment plus fine angled forceps, small spring scissors, microvascular clip.

4. polythene tubing cut to suitable lengths, size appropriate to that of the vessel being cannulated (e.g. for rat 0.58mm internal diameter; 0.96mm outside diameter).
5. dissecting microscope
6. cold light source
7. thermostatically controlled heating blanket, with rectal thermometer

2.3 Blood flow assay

1. ^{125}I-labelled IAP (^{125}I-IAP) and suitable protective equipment
2. minimal dead-space glass syringe
3. general dissecting instruments for excising tissue
4. stop-clock
5. lidded container containing saline-soaked gauze
6. gamma counter and suitable vials for tissue and blood samples
7. analytical balance
8. anaesthetic (see **Note 5**)
9. fraction collector set to collect at 1 second intervals
10. syringe pump for infusion and withdrawal
11. 1000U/ml heparin (use neat for rats and diluted 1 in 10 with saline for mice).
12. injection saline
13. high concentration solution of sodium pentobarbitone e.g. Euthatal™

3. Methods

3.1 Animal preparation

In the rat, a tail artery and vein are most suitable for cannulation. In the mouse, either the carotid artery and jugular vein or femoral artery and vein can be used.

1. Prepare 30 cm lengths of cannulae. For rat use 0.96 mm outside diameter (o.d.); 0.58 mm internal diameter (i.d.). The cannula wall may be shaved down at the tip and the end may be slightly bevelled to aid insertion. Use a microscope to ensure that there are no sharp edges. For mouse use a short length of 0.61 mm o.d.; 0.28 mm i.d. cannula, stretched to a smaller diameter at the tip and connected to a longer length of 0.96 mm o.d.; 0.58 mm i.d. cannula to reduce resistance to flow. Attach each length to a 1 ml syringe filled with heparinised saline.
2. Anaesthetize the animal, insert rectal thermocouple and place on heating blanket. Also, an overhead lamp is a useful additional heat source.
3. Illuminate surgical area with a cold light source.
4. Expose the relevant vessel. For the rat tail, this involves making two 2 cm incisions through the skin, each side of the vessel, approximately 5 mm apart and approximately 2 cm from the base of the tail. Use artery forceps to clear the skin from the underlying connective tissue and cut the skin at the distal end to create a flap (see **Note 6**).
5. Keep exposed vessels moist at all times using warmed saline.
6. Free the vessel from surrounding connective tissue using fine blunt-end forceps.

7. Place two lengths of suture under the vessel, tying off the most distal to the heart, which can be used to apply slight tension to the vessel.
8. Occlude the vessels as far proximal as possible using a microvascular clip.
9. Using spring scissors, make a v-shaped cut in the vessel close to the distal knot and insert cannula. Advance cannula into the vessel approximately 2 cm or more, by removing clip (see **Note 7**).
10. Aspirate gently to ensure that blood is free flowing. It may not be possible to aspirate the vein but a small volume of saline can be injected to check for patency.
11. Tie both sutures securely around the cannula. Use tape or tissue-compatible glue to secure the cannula to the skin distal to the distal suture. Close the wound.

3.2 Blood flow assay

Two alternatives are described; the classic tissue equilibration method for rats and the indicator fractionation method for rats or mice. Graham *et al* (24) directly compared results obtained with these two techniques in a rat brain tumour model and the main advantages and disadvantages of each method are given in Table 1.

3.2.1 Tissue equilibration technique

Cannulation of two tail veins and one tail artery are required, as described above.

1. Remove ^{125}I-IAP from the freezer and bring slowly to room temperature. Using suitable containment and a low dead-space glass syringe, carefully remove required volume ^{125}I-IAP (0.2 – 0.3 MBq per rat) and dispense into a vial.
2. Evaporate the methanol using a very gentle stream of nitrogen and slowly add injection saline to the ^{125}I-IAP (0.8ml per rat plus extra to account for syringe dead spaces etc). Gently mix.
3. Load a syringe of size suitable for infusion with the ^{125}I-IAP solution (needle must be suitable size for the venous cannula).
4. For anaesthetized animals, keep warm, as described above. Check arterial blood pressure and heart rate by connecting the arterial cannula to a pressure transducer and recording device. Then clamp off the cannula and connect it to the fraction collector, loaded with pre-weighed glass tubes, for subsequent blood collection.
5. Inject and flush in 0.1ml neat heparin (= 100 I.U.) via one of the venous cannulae to ensure the blood flows freely from the arterial cannula.
6. Cut one of the venous cannulae to approx. 3 cm in length and connect a syringe containing approx. 0.5ml Euthatal^{TM}. A small “T-connector” may also be used to allow drug administration via this cannula.
7. Set syringe pump speed to 1.6 ml/min (see **Note 8**). Carefully place the ^{125}I-IAP-containing syringe in the pump and connect it to the second venous cannula.

8. Start the stop-clock and unclamp the artery, checking that blood is free-flowing. At 5 s, start syringe pump and fraction collector (see **Note 9**). At 35 s, inject Euthatal^{TM} and stop pump; rapidly excise tissues of interest and stop fraction collector (see **Note 10**). Place tissues in the lidded container to prevent drying. Weigh the blood tubes and cap them. Weigh the tissues and place them in gamma counting tubes.
9. Count the blood and tissue samples on the gamma counter.

3.2.2 Indicator fractionation technique

Cannulations of one artery and two veins are required. Alternatively, cannulae attached to shafts of hypodermic needles can be inserted into tail veins percutaneously instead of cannulating veins.

1. Follow points 1-3 above, preparing 0.07 MBq ^{125}I-IAP in 0.05 ml saline per mouse.
2. For anaesthetized animals, keep warm, as described above. Check arterial blood pressure and heart rate by connecting the arterial cannula to a pressure transducer and recording device.
3. Set syringe pump speed to 150µl/min (mouse) or 1.6 ml/min (rat).
4. Load a 250µl syringe (for mouse) or 2 ml syringe (for rat) with approx 100µl saline, attach a 23G needle and position in the pump.
5. Cut the venous cannula as short as possible and inject 0.05ml of diluted heparin (≡ 5 I.U.) for mouse or 0.1 ml neat heparin (≡ 100 I.U.) for rat. Disconnect heparin syringe and attach ^{125}I-IAP syringe and a syringe

containing injection saline via a T-piece. Connect syringe containing Euthatal™ to second venous cannula.

6. Clamp the artery cannula, disconnect it from the pressure transducer, and connect it to the syringe pump. Ensure that the pump is set to withdraw and allow it to withdraw very briefly to ensure that the cannula is patent and the syringe is positioned correctly.
7. Start the stop-clock and pump simultaneously. Check that the blood is flowing freely. At 3 s, inject 0.05 ml of ^{125}I-IAP for mouse or 0.2 ml for rat, as a rapid bolus via the venous cannula, followed immediately by 0.05 ml saline from the second syringe. At 13 - 18 s (see **Note 11**), inject Euthatal™ and immediately pull out full length of arterial cannula and excise the tissue of interest. All the blood should be retained in the cannula. Place the tissue in a pre-weighed gamma counting tube.
8. Attach a saline filled syringe to the arterial cannula and eject all the blood into a gamma counting tube together with 1ml of saline.
9. Count the blood and tissue samples on the gamma counter.

3.3 Blood flow analysis

3.3.1 Tissue equilibration technique

1. Analysis is based on a model which assumes a vascular compartment from which the input function derives and a single (extra-vascular) well-mixed tissue compartment (Figure 1). A small, highly soluble and inert tracer, such as IAP, is assumed to rapidly equilibrate between all blood components and the tissue

compartment. In this case, the model based on Kety (25) describes the relationship between the tissue concentration of the tracer at time *t*, $C_t(t)$, and the arterial blood concentration of the tracer at time *t*, $C_a(t)$, by the Equation:

$$C_{tiss}(t) = k_1 C_a(t) \otimes exp(-k_2 t) \quad \text{.....Equation (2)}$$

where k_1 is tissue blood flow rate (F) and k_2 is $k_1 / \alpha\lambda$; α is the effectively perfused fraction of tissue (i.e. the fraction of tissue that is immediately accessible to the tracer) and λ is the equilibrium partition coefficient of the tracer between tissue and blood; $\otimes$ denotes the convolution integral; in imaging studies, $\alpha\lambda$ is often referred to as the apparent volume of distribution (VD_{app}) of the tracer in the tissue (26), $C_{tiss}(t)$ and $C_a(t)$ are expressed in radioactivity counts per g tissue and per ml blood respectively, using 1.05 for the density of blood.

2. In this method, $C_{tiss}(t)$ is measured at only one time-point i.e. after tissue excision. Hence only one parameter, k_1 (F) can be estimated from the data (see **Note 12**). λ is approximated from literature values or estimated from separate experiment (27) and α is taken as 1.0 (see **Notes 12** and **13**). Studies have shown that the method is relatively insensitive to small changes in λ because of the short time-scale of the experiment (28). Also see Table 1.
3. Solving Equation (2): Data can be fitted to Equation (2) using a simple 'Table Lookup Method'. In this method, since the input function is known, then the expected tissue activity at the time of excision $C_{tiss}(T)$ can be calculated for

each of a range of realistic values of *F*, using Equation (2). Direct comparison of the observed C_{tiss} *(T)* against the table then gives the required estimate of *F* (Figure 2). Evaluation of the Integral in Equation (2) requires a numerical integration routine, which are commonly available in statistical analysis packages, or can be programmed using computer applications such as MATLAB (The Mathworks, USA ©). A further issue, which needs to be taken into account when assessing the accuracy of this type of technique, is the possibility that the input function time course may not be accurately measured because of a time delay between the radioactivity reaching the tissue and reaching the blood collection tubes and because of smearing or dispersion effects occurring on the arterial cannula before blood collection. These delay and dispersion effects can be corrected for (see **Note 14**) but do add further complication to the analysis.

3.3.2 Indicator Fractionation technique

1. This method was first used by Goldman & Sapirstein (29), with later modifications (30). It simplifies the model used in *Equation 2* by assuming that the backflux of the tracer from tissue into the blood is negligible compared with its influx into the tissue, for a short period of time after injection of the tracer (see **Note 15**). Under these conditions, Equation 2 reduces to:

$$k_1 = C_{tiss}(T) / \int_0^T C_a(t)dt \quad \text{.....Equation (3)}$$

where k_1, *t*, $C_a(t)$ are as defined above and $C_{tiss}(T)$ is concentration of tracer in the tissue at the end of the experiment (at time $t = T$).

2. T is typically set at 10 –15 seconds, during which time collection of sufficient blood samples, as described for the tissue equilibration technique, is difficult. Instead, the constant withdrawal technique can be used. Here, blood is withdrawn from an artery at a constant rate using a pump from $t = -T'$ to $t = T$, where $-T'$ is the time at which the pump is started. A bolus injection of tracer is given at $t = 0$. Under these conditions,

$$\int_0^T C_a(t)dt = C_c\,(T + T') = C_c V_b/r = X/r \quad \text{.....Equation (4)}$$

where C_c is mean concentration of tracer in the blood sample; V_b is volume of blood collected; X is total radioactive counts in the collected blood sample and r is rate of withdrawal of blood.

3. X/r can be substituted into Equation 3 and blood flow rate, k_1, can be calculated from a knowledge of the counts, X, pump rate, r, and concentration of the tracer in the tissue at the end of the experiment, $C_{tiss}\,(T)$. As for the tissue equilibration technique, there are inaccuracies in the measurement of the input function using this technique, associated with delay and dispersion along the plastic cannula. However, the constant withdrawal method means that definition of a concentration-time curve is not required and only the last part of the actual arterial time-course is lost by the blood sampling method. In addition, the experimental set-up of the indicator fractionation method means that the arterial cannula can be kept short, minimizing the delay involved.

3.3.3 Comparison of the two blood flow methods

The advantages and disadvantages of the classic tissue equilibration method and the indicator fractionation method are summarized in Table 1. Patlak *et al*. (28) carried out an evaluation of errors involved in the two techniques, which can be summarized as follows:

1. Errors in the tissue equilibration method are minimized if an optimal infusion schedule is used (a ramped schedule is best but a constant infusion is reasonable), timing is measured precisely and corrections are made for delay and dispersion. Under these conditions, 10-15% inaccuracy in the value used for λ is well tolerated in the calculation of *F*. If precise measurement of λ can be made, this is the method of choice.
2. If λ cannot be measured reasonably accurately, the indicator fractionation technique maybe the better option for estimating *F*. Errors associated with backflux are minimized by a short experimental time. Errors associated with imprecise timing are minimized by bolus administration of the tracer (so that arterial concentration is low at tissue excision). The constant withdrawal method is an added advantage for its simplicity and accuracy. However, backflux cannot be completely prevented (especially with bolus administration) and may introduce significant errors where *F* is high and/or α is low. Delay and dispersion effects are reasonably well tolerated.
3. Both techniques require accurate measurement of tracer concentration in the tissue (C_{tiss}).

4. Notes

1. The methodology presented here is based on a single tissue compartment model. This can be derived from the classic Renkin-Crone unit capillary model (31, 32), which gives an explicit relationship between flow, the extraction of substances from blood into tissue and the mean permeability surface area product of the capillary bed. Recent simulation studies show that the degree of local heterogeneity in capillary architecture and transit times of blood through the capillaries may also affect the precise relationship between flow and extraction of substances from the blood into tissue (33, 34).
2. The basic experimental principles and analytical methods described here also apply to various external imaging techniques that are now available for use in small animals e.g. positron emission tomography (35). These techniques allow repeated evaluation of blood flow rate (and other pharmacodynamic end-points) in the same animal, as long as the biological and radioactive half-lives of the tracer are compatible with the time-scale of the experiment. In addition they allow definition of more than one vascular parameter (see note 12 below).
3. Instead of obtaining a single value for the blood flow rate within a tissue (usually by calculating C_{tiss} from gamma counts of tissue activity), the variation of blood flow rate within a tissue can be obtained at high spatial resolution (~ 50 µm) by using a radiotracer that is suitable for autoradiography or phosphor imaging (Figure 2). In these cases, C_{tiss} is

obtained in raster fashion across tissue sections for calculation of corresponding k_1 (F) values (36).

4. Local radiation safety procedures need to be followed for all the techniques described to avoid contamination of personnel and equipment.
5. General anaesthesia seriously affects mean arterial blood pressure in rodents, especially in mice, and its effects on tissue blood flow rates need to be considered in planning experiments. Animals can be allowed to recover from general anaesthesia induced by inhalational anaesthetics following cannulation but, in this case, procedures for preventing cannula disturbance and minimising pain and distress to the animals need to be implemented (37).
6. Tail cannulations: the tail artery lies relatively deep within a cleft in the cartilage and requires an incision to be made through the overlying connective tissue for it to be accessible. Once freed it is robust for cannulation; the vein is much more superficial and easily located, although more fragile than the artery and liable to constriction and tearing.
7. A topical vasodilator such as procaine can be used to aid cannula insertion.
8. Volumes of saline solutions of IAP for intravenous administration are chosen to compensate for rate of blood loss during the course of the experiments.
9. A constant infusion schedule for delivery of the radiotracer is described, as it is simple to achieve in practice. However, an infusion schedule that

increases with time (ramped) could be employed because this reduces the influence of an incorrect value for λ, on the calculated value of *F* (28). The movement of the fraction collector and the infusion/withdrawal rates of the pump need to be carefully calibrated prior to experiments.

10. Timing errors can be significant if blood flow to tissues of interest is not stopped at the instant that the pump is stopped. Also see Table 1.
11. A short duration increases timing errors but a longer one increases errors associated with backflux of the tracer from the tissue into blood. Also see Table 1.
12. A disadvantage of this particular technique is that the tissue concentration of the tracer is assayed at only one time point. Hence, as noted above, only one parameter (*F*) can be estimated, whereas values for α and λ have to be assumed. Other, more sophisticated techniques involving non-invasive imaging, such as PET (see note 2), involve a full time course of the tissue to be assayed, allowing estimation of $\alpha\lambda$ (VD_{app}) for example, as well as *F*. This is of particular interest in the case of tumour blood flow, where the effectively perfused tissue fraction (α) (i.e. the fraction of tissue that is immediately accessible to the tracer) is often less than 1.0 because of large intercapillary distances or ischaemic regions (26). However, the spatial resolution of non-invasive imaging cannot compete with the high spatial resolution achievable with the invasive techniques described here (see note 3). In the invasive technique, α is usually assumed to be 1.0. If it is actually less than 1.0, for a sampled tissue region of interest, the

measured tissue concentration of the tracer, C_{tiss}, will be low because it is averaged over the whole region, including the inaccessible part. Thus the calculated value of F will reflect average blood flow for the region and underestimate that of the perfused tissue fraction.

13. Beyond the short time-scale of these experiments, IAP redistributes in tissue in a space-dominated rather than a flow-dominated pattern. At equilibrium, IAP might be expected to distribute in proportion to the tissue water content, such that λ would be similar in all tissues and close to 1.0. However, experimental evidence indicates that, although λ for IAP is close to 1.0 in many tissues, it is somewhat variable (27). This may relate to its high lipid solubility or it may be a reflection of problems in accessing true values of λ because of loss of the radioactive label from the molecule at long times (hours) after injection.

14. A simple model which can be used to describe dispersion effects is given by the equation:

$$C_m(t) = C_a(t) \otimes k_d \exp(-k_d t) \quad \text{.....Equation (5)}$$

where $C_m(t)$ is the measured tracer concentration at the cannula outflow, $C_a(t)$ is the inflow concentration and k_d (min^{-1}) is a dispersion constant, which is dependent on flow rate, length and internal diameter of the cannula and the interaction with blood on its internal surface. k_d for a particular cannula and flow rate of blood can be calculated from Equation (5), if experiments are undertaken *in vitro* whereby the blood pumped through a cannula at a particular rate is switched rapidly between labelled

blood and unlabelled blood and the dispersion effect measured in the outflow. Results from such an experiment are presented in Table 2. Delay (t_d) can be estimated directly from the known volume of the cannula and the blood flow rate down the cannula. These values for k_d and t_d can be incorporated in Equation 2 to give a working form of the Equation:

$$C_{tiss}(t) = (k_1/k_d)C_m(t+t_d) + (1-k_2/k_d)k_1C_m(t+t_d) \otimes \exp(-k_2t) \quad \text{Equation (6)}$$

If dispersion effects are small i.e. large k_d, then this Equation reduces to Equation 2. If dispersion effects are marked, i.e. small k_d, then the Equation illustrates that failing to take dispersion effects into account has a marked effect on estimates of *F*. These issues were first quantitatively described by Meyer (38) (but note that a dispersion time constant equivalent to $1/k_d$ was used in this case).

15. In addition to using a short experimental time, *T*, errors associated with backflux in this technique are minimized if blood flow rate is low and there is a big accessible space in the tissue for the tracer (high α). Note that the short T gives the potential for large timing errors and great care must be taken to time the experiment accurately. As for the tissue equilibration technique, this means that blood flow to tissues needs to be stopped precisely at T. Interestingly, timing errors appear to be less of an issue with this technique than with the tissue equilibration technique for measurement of cerebral blood flow rate (28).

References

1. Stewart, G. N. (1894) Researches on the circulation time in organs and on the influences which affect it. *J Physiol (London)* 15, Parts I-III.
2. Reyes-Aldasoro, C. C., Akerman, S., Tozer, G. M. (2008) Measuring the velocity of fluorescently labelled red blood cells with a keyhole tracking algorithm. *J Microscopy* 229, 162-173.
3. Intaglietta, M., Tompkins, W. R. (1973) Microvascular measurements by video image shearing and splitting. *Microvasc Res* 5, 309-312.
4. Fontanella, A. N., Schroeder, T., Hochman, D. W., Chen, R. E., Hanna, G., Haglund, M. M., Secomb, T. W., Palmer, G. M., Dewhirst, M. W. (2013) Quantitative mapping of hemodynamics in the lung, brain, and dorsal window chamber-grown tumors using a novel, automated algorithm. *Microcirculation* 20, 724-735.
5. Brizel, D. M., Klitzman, B., Cook, J. M., Edwards, J., Rosner, G., Dewhirst, M. W. (1993) A comparison of tumor and normal tissue microvascular hematocrits and red cell fluxes in a rat window chamber model. *Int. J. Radiat. Oncol. Biol. Phys.* 25, 269-276.
6. Tozer, G. M., Prise, V. E., Wilson, J., Cemazar, M., Shan, S., Dewhirst, M. W., Barber, P. R., Vojnovic, B., Chaplin, D. J. (2001) Mechanisms associated with tumor vascular shut-down induced by combretastatin a-4 phosphate: Intravital microscopy and measurement of vascular permeability. *Cancer Res* 61, 6413-6422.
7. Oye, K. S., Gulati, G., Graff, B. A., Gaustad, J. V., Brurberg, K. G., Rofstad, E. K. (2008) A novel method for mapping the heterogeneity in blood supply to normal and malignant tissues in the mouse dorsal window chamber. *Microvasc Res* 75, 179-187.
8. Stern, M. D. (1975) In vivo evaluation of microcirculation by coherent light scattering. *Nature* 254, 56-58.
9. Smith, K. A., Hill, S. A., Begg, A. C., Denekamp, J. (1988) Validation of the fluorescent dye hoechst 33342 as a vascular space marker in tumours. *Br J Cancer* 57, 247-253.
10. Hill, S. A., Tozer, G. M., Chaplin, D. J. (2002) Preclinical evaluation of the antitumour activity of the novel vascular targeting agent Oxi 4503. *Anticancer Res* 22, 1453-1458.
11. Lunt, S. J., Akerman, S., Hill, S. A., Fisher, M., Wright, V. J., Reyes-Aldasoro, C. C., Tozer, G. M., Kanthou, C. (2011) Vascular effects dominate solid tumor response to treatment with combretastatin A-4-phosphate. *Int J Cancer* 129, 1979-1989.
12. Chalkley, H. W. (1943) Method for quantitative morphologic analysis of tissues. *J Natl Cancer Inst* 4, 47-53.
13. Vermeulen, P. B., Gasparini, G., Fox, S. B., Colpaert, C., Marson, L. P., Gion, M., Belien, J. A., de Waal, R. M., Van Marck, E., Magnani, E., Weidner, N., Harris, A. L., Dirix, L. Y. (2002) Second international

consensus on the methodology and criteria of evaluation of angiogenesis quantification in solid human tumours. *Eur J Cancer* 38, 1564-1579.
14. Weiskoff, R. M. (1993) Pitfalls in MR measurement of tissue blood flow with intravascular tracers: Which mean transit time? *MRM* 29, 553-559.
15. Messmer, K. (1979) Radioactive microspheres for regional blood flow measurements. Actual state and perspectives. *Bibl Anat* 18, 194-197.
16. Jirtle, R. L. (1980) Blood flow to lymphatic metastases in conscious rats. *Eur J Cancer* 17, 53-60.
17. Jirtle, R. L., Hinshaw, W. M. (1981) Estimation of malignant tissue blood flow with radioactively labelled microspheres. *Eur J Cancer Clin Oncol* 17, 1353-1355.
18. Sapirstein, L. A. (1958) Regional blood flow by fractional distribution of indicators. *Am J. Physiol.* 193, 161-168.
19. Obrist, W. D., Thompson, H. K., King, C. H. and Wang, H. S. (1967) Determination of regional cerebral blood flow by inhalation of 133-xenon. *Circ Res* 20, 124-135.
20. Young, W. (1980) H2 clearance measurement of blood flow: A review of technique and polarographic principles. *Stroke* 11, 552-564.
21. Sakurada, O., Kennedy, C., Lehle, J., Brown, J. D., Carbin, J. L., Sokoloff, L. (1978) Measurement of local cerebral blood flow with iodo [^{14}C] antipyrine. *Am. J. Physiol.* 234, H59-H66.
22. Tozer, G. M., Shaffi, K. M. (1993) Modification of tumour blood flow using the hypertensive agent, angiotensin II. *Br. J. Cancer* 67, 981-988.
23. Trivedi, M. A. (1996) A rapid method for the synthesis of 4-iodoantipyrine. *J Labelled Comp Radiopharm* 38, 489-496.
24. Graham, M. M., Spence, A. M., Abbott, G. L., O'Gorman, L., Muzi, M. (1987) Blood flow in an experimental rat brain tumor by tissue equilibration and indicator fractionation. *J Neuro-Oncol* 5, 37-46.
25. Kety, S. S. (1960) Theory of blood tissue exchange and its application to measurements of blood flow. *Methods Med. Res.* 8, 223-227.
26. Tozer, G. M., Shaffi, K. M., Prise, V. E., Cunningham, V. J. (1994) Characterisation of tumour blood flow using a "tissue-isolated" preparation. *Br. J. Cancer* 70, 1040-1046.
27. Tozer, G. M., Morris, C. (1990) Blood flow and blood volume in a transplanted rat fibrosarcoma: Comparison with various normal tissues. *Radiother Oncol* 17, 153-166.
28. Patlak, C. S., Blasberg, R. G., Fenstermacher, J. D. (1984) An evaluation of errors in the determination of blood flow by the indicator fractionation and tissue equilibration (Kety) methods. *J. Cerebr Blood Flow Metab* 4, 47-60.
29. Goldman, H., Sapirstein, L. A. (1973) Brain blood flow in the conscious and anaesthetized rat. *Am. J. Physiol.* 224, 122-126.
30. Gjedde, S. B., Gjedde, A. (1980) Organ blood flow rates and cardiac output of the Balb/c mouse. *Comp Biochem Physiol* 67A, 671-674.
31. Renkin, E. M. (1959) Transport of potassium-42 from blood to tissue in isolated mammalian skeletal muscles. *Am J Physiol* 197, 1205-1210.

32. Crone, C. (1963) The permeability of capillaries in various organs as determined by use of "indicator diffusion" method. *Acta Physiol. Scand.* 58, 292-305.
33. Jespersen, S. N., Ostergaard, L. (2012) The roles of cerebral blood flow, capillary transit time heterogeneity, and oxygen tension in brain oxygenation and metabolism. *J Cerebr Blood flow Metab* 32, 264-277.
34. Ostergaard, L., Tietze, A., Nielsen, T., Drasbek, K. R., Mouridsen, K., Jespersen, S. N., Horsman, M. R. (2013) The relationship between tumor blood flow, angiogenesis, tumor hypoxia, and aerobic glycolysis. *Cancer Res* 73, 5618-5624.
35. Herrero, P., Kim, J., Sharp, T. L., Engelbach, J. A., Lewis, J. S., Gropler, R. J., Welch, M. J. (2006) Assessment of myocardial blood flow using 15O-water and 1-11C-acetate in rats with small-animal pet. *J Nucl Med* 47, 477-485.
36. Tozer, G. M., Prise, V. E., Wilson, J., Locke, R. J., Vojnovic, B., Stratford, M. R. L., Dennis, M. F., Chaplin, D. J. (1999) Combretastatin a-4 phosphate as a tumor vascular-targeting agent: Early effects in tumors and normal tissues. *Cancer Res.* 59, 1626-1634.
37. Richardson, C. A., Flecknell, P. A. (2005) Anaesthesia and post-operative analgesia following experimental surgery in laboratory rodents: Are we making progress? *Altern Lab Anim* 33, 119-127.
38. Meyer, E. (1989) Simultaneous correction for tracer arrival delay and dispersion in CBF measurements by the H215O autoradiographic method and dynamic PET. *J Nucl Med* 30, 1069-1078.

Figure Legends

Figure 1

Chemical structure of 4-Iodo[*N-methyl*-^{14}C]antipyrine (a) and the compartmental model used for the quantitative estimation of *F* (b). When the extraction fraction, *E*, of a blood-borne tracer is 1.0, the rate constant k_1 represents *F*. k_2 represents the back-flux and C_a and C_{tiss} represent the arterial blood and tissue concentrations of the tracer respectively. In this model, the tissue is a single well-mixed compartment.

Figure 2

Estimation of tissue blood flow rate (*F*) in the P22 rat sarcoma and several normal rat tissues using the tissue equilibration method with ^{125}I-IAP (a) and ^{14}C-IAP (b). Results in panel a) were obtained by calculating C_{tiss} from gamma counts of large tissue samples. Data shows effects of the vascular disrupting agent combretastatin A4-P and the nitric oxide synthase inhibitor L-NNA plus the combination of the two. * represents a significant difference between treated and control untreated tumours. The image in panel b) was obtained from an untreated P22 tumour by calculating multiple values for C_{tiss} from quantitative autoradiography of tumour sections. The mean *F* is 3.8 ml•g^{-1}•min^{-1}. The image in panel c) illustrates the vascular networks in the P22 tumour obtained by multi-photon fluorescence microscopy.

Figure 1

Tozer, Prise & Cunningham

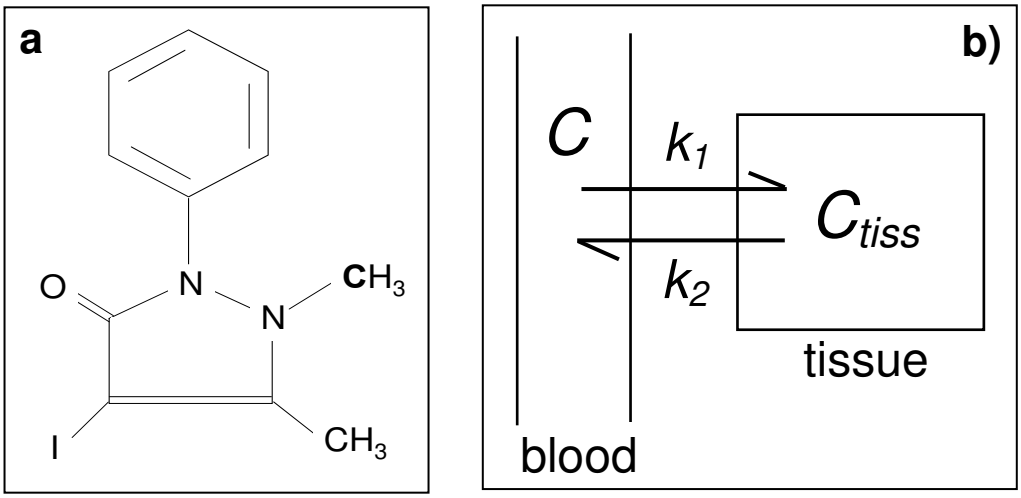

Figure 2

Tozer, Prise and Cunningham

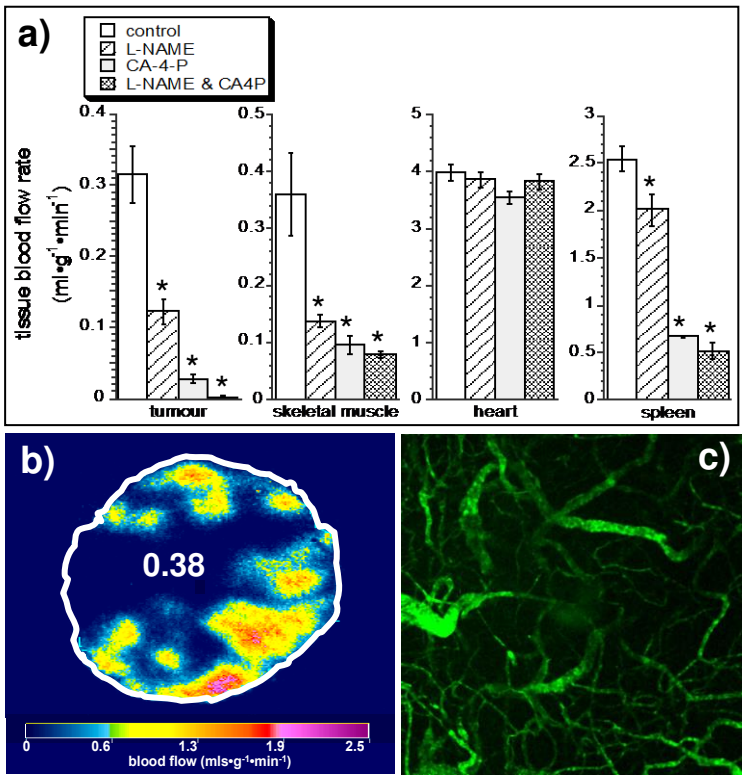

Table 1: Comparison of radiotracer methods for estimation of tissue blood flow rate (*F*)

Tissue Equilibration Technique	Indicator Fractionation Technique
Requires blood vessel cannulation	Requires blood vessel cannulation
Time-consuming	Relatively easy to perform
Calculations require curve fitting algorithms	Calculations require only a simple formula
Backflux is taken into account in the model	Very sensitive to errors associated with backflux
Relatively sensitive to timing errors and delay & dispersion effects	Reasonably tolerant of timing errors and delay & dispersion effects
Reasonably tolerant of imprecision in λ	Tolerant of imprecision in λ
Method of choice where λ is well-defined	Method of choice where λ is ill-defined, especially if F is low and α large

Table 2 : Example of expressions used to calculate the dispersion constant k_d (min^{-1}) from the linear speed (ν in cm per min) of blood flowing down various types of cannulae. These expressions were obtained by pumping blood at several known flow rates through each type of cannula and rapidly switching between labelled and unlabelled blood. The time-activity curves for the blood flowing out of the cannulae were compared with the known inflow time-activity curves, using Equation 5, to estimate k_d for each condition. The relationship between k_d and ν was described by the equation for a straight line, as shown. The cannulae used were prepared from Portex™ low density polyethylene tubing.

TYPE OF CANNULA	200 mm length	300 mm length
0.50 mm internal diameter	$6.72 + 0.048 * \nu$	$3.84 + 0.036 * \nu$
0.58 mm internal diameter	$9.54 + 0.040 * \nu$	$-0.6 + 0.042 * \nu$